Exact Finite Element Method Analysis of Viscoelastic Tapered Structures to Transient Loads

Constantine Chris Spyrakos

N88-13632

A general method is presented for determining the dynamic torsional/axial response of linear structures composed of either tapered bars or shafts to transient excitations. The method consists of formulating and solving the dynamic problem in the Laplace transform domain by the finite element method and obtaining the response by a numerical inversion of the transformed solution. The derivation of the torsional and axial stiffness matrices is based on the exact solution of the transformed governing equation of motion, and it consequently leads to the exact solution of the problem. The solution permits treatment of the most practical cases of linear tapered bars and shafts, and employs modelling of structures with only one element per member which reduces the number of degrees of freedom involved. The effects of external viscous or internal viscoelastic damping are also taken into account.

INTRODUCTION

The static dynamic and stability analysis of nonuniform structures composed of tapered beams and/or bars has attracted considerable attention (Chu et. al. 1970; Kounadis 1975; Sato 1980). A thorough presentation of developments pertinent to the dynamic behavior of tapered beams/bars has been presented by Kolousek (1973). Lately, GangaRao and Spyrakos (1986) determined the static and dynamic response of tapered flexural/axial members through an analytical technique applicable to the wide class of initial-boundary value problems governed by linear differential operators with variable coefficients. Besides analytical methods restricted to limited cases due to the involved equations of motion and the associated conditions, numerical methods such as the Finite Difference Method (FDM) (Liable 1985) and especially the Finite Element Method (FEM), have been successfully employed (Gallagher et al. 1970; Rough et al. 1979). The FEM appears to be more popular than the FDM since it presents several organizational advantages and handles boundary conditions easier. Use of the FEM has been primarily based on the approximate lumped or consistent mass representation and on displacement functions which are solutions of the static governing equations (Beaufait et al. 1970; Gupta 1985). Tapered members are considered as an assembly of uniform elements with known stiffnesses which are super-imposed to construct the stiffness of the

PRECEDING PAGE BLANK NOT FILMED

member. This stepped representation requires a relatively large number of elements to accurately determine the dynamic response. In the case of linearly tapered members, an alternative approach would be the use of exact stiffness matrices developed from the solution of the static governing equation of axial/flexural deformation (Just 1977; Holzer 1986). Recently, Banerjee and Williams (1986) developed exact dynamic stiffness matrices for the axial, torsional, and flexural vibration of tapered beams to harmonically varying forces. The approximate as well as the exact stiffness matrices developed by Banerjee can be used in a conventional modal analysis formulation to provide the response of tapered structures. Such an analysis, however, requires prior determination of the natural frequencies and nodal shapes that can be obtained by solving the free vibration problem (Bathe 1982). Alternative highly accurate and efficient FEM formulations, based on transformed dynamic stiffness matrices, have been successfully employed by Spyrakos and Beskos, (1982) and Tamma et. al. (1987) for the dynamic analysis of frameworks modelled with uniform elements and subjected to general transient forces. In their analysis, the transformed dynamic stiffness matrices were developed through application of either Fourier or Laplace transform with respect to time on the equation of motion of a beam element. The structural response in the time domain is obtained from the transformed stiffness equation and a numerical inversion. Therefore, such an approach retains the advantages of the direct stiffness method eliminating the need for prior solution of an eigenvalue problem.

In this paper, the dynamic response of structures composed of tapered bars and shafts to transient axial and/or torsional forces is determined. The formulation considers the most practical cases of cross-sections and types of taper, and includes effects of both external viscous and internal viscoelastic damping. The analysis employs the FEM with dynamic stiffness matrices expressed in the Laplace transform domain. The derivation of the stiffness matrices is based on the exact solution of the axial or torsional tapered element governing equations expressed in terms of Bessel functions. Thus, modelling of the structure requires only one element per member which reduces the number of degrees of freedom involved and simplifies the modelling of the configuration. Furthermore, evaluation of the response from the stiffness equation leads to the "exact" solution of the problem. A numerical Laplace transform based on Durbin's algorithm (Durbin 1974) is then used to determine the structural response in the time domain. Durbin's algorithm was chosen since it allows an efficient and accurate direct and inverse numerical Laplace transform of general forcing functions (Beskos et al. 1983).

FORMULATION OF THE PROBLEM

Consider the general tapered bar element a-b with a straight centroidal axis and directions of the principal axes being the same for all cross sections as shown in Figure 1. The variation of the cross-sectional area $A(x)$ and polar second moment of area $J(x)$ may be represented as

$$A(x) = A_a \left(1 + r \frac{x}{L}\right)^m$$

and $\qquad$ (1)

$$J(x) = J_a (1 + r \frac{x}{L})^{m+2},$$

where L is the length of the element and A_a, J_a denote the values of the cross-sectional area and polar second moment of area, respectively, at the cross-section a in Figure 1. Given the geometrical properties of the element at the end sections (a and b), the positive constants r and m can be evaluated from the expressions

and
$$r = \left(\frac{A_a J_b}{A_b J_a} \right)^{1/2} - 1$$

$$m = 2 \ln \left(\frac{A_b}{A_a} \right) / \left(\ln \frac{J_b A_a}{J_a A_b} \right)^{-1} \qquad (2)$$
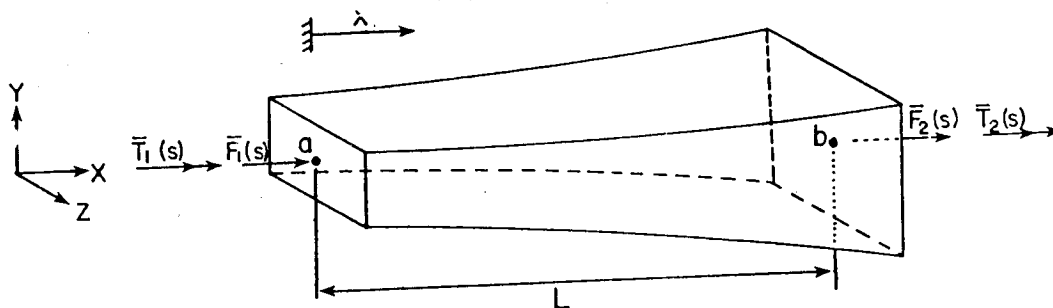

Figure 1. Geometry and sign convention of a general bar/shaft element

Even though the developments presented in the following sections are valid for any value of m from equation (2), special emphasis will be placed on the practical cases of linear taper with m=1 and m=2. The case of m=1 corresponds to rectangular and I-sections, while m=2 pertains to circular as well as I-sections (Gupta 1985).

Axial Vibration

The equation of motion for a small amplitude, free axial vibration of a linear elastic tapered bar (m=1) is

$$\frac{\partial}{\partial x} [EA(x) \frac{\partial u}{\partial x}] - \rho A(x) \frac{\partial^2 u}{\partial t^2} = 0, \qquad (3)$$

where $u = u(x,t)$ is the axial displacement of the bar and E, ρ are the modulus of elasticity and the mass density of the bar, respectively. Expressing, $A(x)$ in terms of $\xi = 1 + r \frac{x}{L}$ equation (3) takes the form

$$\frac{\partial^2 u}{\partial \xi^2} + \frac{m}{\xi} \frac{\partial u}{\partial \xi} - \frac{\rho L^2}{Er^2} \frac{\partial^2 u}{\partial t^2} = 0 \tag{4}$$

The Laplace transform $\bar{y}$ (s) of a function y(t) is defined by

$$\bar{y}(s) = \int_0^\infty y(t) \, e^{-st} dt \tag{5}$$

where s is, in general, a complex number. Application of the Laplace transform with respect to time on equation (4), under the assumption of zero initial conditions, yields

$$\xi^2 \bar{u}'' + m \xi \bar{u}' - s^2 \frac{\rho L^2}{Er^2} \xi^2 \bar{u} = 0, \tag{6}$$

where primes indicate differentiation with respect to the spatial variable ξ. The general solution of equation (6) can be obtained on the basis of the procedure indicated by Myers (1971). The resulting expression contains Bessel functions of the second kind with complex kernels which are not readily applicable for a concise development of an element stiffness matrix. Thus, after some algebraic manipulations and use of properties of Bessel functions (Abramovitz et al. 1965), one can arrive at the following concise form of the general solution:

$$\bar{u}(s) = \xi^k \{ C_1 I_k (\frac{sL}{r} (\frac{\rho}{E})^{1/2} \xi) + C_2 K_k (\frac{sL}{r} (\frac{\rho}{E})^{1/2} \xi) \}, \tag{7}$$

where C_1 and C_2 are constants and $k = \frac{1-m}{2}$.

Adapting as positive directions of the nodal displacements and forces the ones shown in Figure 1, the evaluation of the axial stiffness matrix for the bar element a-b can be obtained by relating the axial displacements at the nodes a and b to the axial forces

$$\bar{F}_1(s) = -(EA_a \frac{r}{L}) \frac{d\bar{u}}{d\xi} \Big|_{\xi=1} \text{ and } \bar{F}_2(s) = (EA_b \frac{r}{L}) \frac{d\bar{u}}{d\xi} \Big|_{\xi=1+r}$$

through the displacement function $\bar{u}(s)$ given by equation (7) (Spyrakos et al. 1982). An entry $\bar{k}_{ij}$, through Laplace transformed stiffness matrix, is defined as the transformed force at the ith degree of freedom due to a unit transformed displacement at the jth degree of freedom while all the other transformed displacements are zero. Thus, with the sign convention of Figure 1, the following element transformed nodal force-displacement relationship in terms of the dynamic stiffness influence coefficients $\bar{k}_{ij}$ coefficients can be obtained

$$\left\{ \begin{array}{c} \bar{F}_1(s) \\ \bar{F}_2(s) \end{array} \right\} = \left[\begin{array}{cc} \bar{k}_{11} & \bar{k}_{12} \\ \bar{k}_{21} & \bar{k}_{22} \end{array} \right] \left\{ \begin{array}{c} \bar{u}_1 \\ \bar{u}_2 \end{array} \right\}, \tag{8}$$

where

$$\bar{k}_{11} = -H \{I_k(b)K_n(a) + I_n(a) K_k(b)\}$$

$$\bar{k}_{12} = \bar{k}_{21} = \frac{H}{a(1+r)^k} \tag{9}$$

$$\bar{k}_{22} = -H (1+r)^m \{I_n(b) K_k(a) + I_k(a) K_n(b)\}$$

with A, a, b and n given by

$$n = -\frac{1}{2}(1+m), \quad H = \frac{EA_a}{B} s(\rho/E)^{1/2}, \quad a = \frac{sL}{r}(\rho/E)^{1/2}$$

$$b = (1+r)a, \quad B = I_k(a) K_k(b) - I_k(b) K_k(a) \tag{10}$$

For the case $m = 2$, the stiffness influence coefficients can be expressed in terms of hyperbolic functions through the relationships (Abramovitz et al. 1965)

$$I_{-1/2}(z) = (2/\pi z)^{1/2} \cosh z$$

$$K_{-1/2}(z) = e^{-z}(\pi/2z)^{1/2} \tag{11}$$

Thus, after some computational effort, equations (9) take the form

$$\bar{k}_{11} = -\bar{H} \{\cosh(ar) + a^{-1} \sinh(ar)\}$$

$$\bar{k}_{12} = \bar{K}_{21} = \bar{H} (1 + r) \tag{12}$$

$$\bar{k}_{22} = -\bar{H} (1+r)^2 \{\cosh(ar) - b^{-1}\sinh(ar)\} ,$$

where

$$\bar{H} = \frac{EA_a}{\bar{B}} s(\rho/E)^{1/2} \quad \text{and} \quad \bar{B} = -\sinh^{-1}(ar) \tag{13}$$

It should be noted that the dynamic stiffness influence coefficients $\bar{D}_{ij}$ presented by Beskos and Narayanan (1983) for a uniform bar element can be easily deduced from equations (12) and (13) for a=b and r tending to zero.

Torsional Vibration

The equation of motion for free tortional vibration of a linear elastic tapered shaft with circular cross-sections is

$$\frac{\partial}{\partial x}\{GCJ(x) \frac{\partial\phi}{\partial x}\} - \rho J(x) \frac{\partial^2\phi}{\partial t^2} = 0, \tag{14}$$

where $\phi(x,t)$ is the angular displacement, G is the shear modulus, and C, which is equal to one for circular cross-sections represents the torsional rigidity of the cross-section. When C is given appropriate values, equation (14) can also be utilized to approximate the torsional response of a number of other cross-sections. Substituting J(x) given by equation (2) and expressing x in terms of ξ, equation (14) results

$$\frac{\partial^2 \phi}{\partial \xi^2} + \frac{m+2}{\xi} \frac{\partial \phi}{\partial \xi} - \frac{\rho L^2}{CGr^2} \frac{\partial^2 \phi}{\partial t^2} = 0 \tag{15}$$

Application of Laplace transform on equation (15) leads to

$$\xi^2 \bar{\phi}'' + (m+2) \xi \bar{\phi}' - s^2 \frac{\rho L^2}{CGr^2} \xi^2 \bar{\phi} = 0 \tag{16}$$

Observing the similarity between the equations of motion (6) and (16) and following the procedure employed for the treatment of the axial vibration, one can obtain the tortional stiffness equation

$$\begin{Bmatrix} \bar{T}_1(s) \\ \bar{T}_2(s) \end{Bmatrix} = \begin{bmatrix} \bar{k}_{11} & \bar{k}_{12} \\ \bar{k}_{21} & \bar{k}_{22} \end{bmatrix} \begin{Bmatrix} \bar{\phi}_1 \\ \bar{\phi}_2 \end{Bmatrix}, \tag{17}$$

where the dynamic stiffness influence coefficients $\bar{k}_{ij}$ can be determined from equation (9) by replacing the variables m, a, b and H with ℓ, α, β and D, respectively, given by

$$\ell = m+2, \quad \alpha = \frac{sL}{r} \left(\frac{\rho}{CG} \right)^{1/2}$$

$$\beta = (1+r)\alpha, \quad D = CGJ_a s \left(\frac{\rho}{CG} \right)^{1/2} /B \tag{18}$$

The positive directions of the nodal torsions and angular displacements are depicted in Figure 1.

For the case m = 2, the dynamic stiffness influence coefficients $\bar{k}_{ij}$ can be expressed in terms of hyperbolic functions with the aid of expressions (11). Thus,

$$\bar{k}_{11} = -\bar{D} \left\{ \sinh(\alpha r) \left[\frac{3}{\alpha} - \frac{1}{\beta} - \frac{3}{\alpha^2 \beta} \right] + \cosh(\alpha r) \left[1 + \frac{3}{\alpha^2} - \frac{3}{\alpha \beta} \right] \right\}$$

$$\bar{k}_{12} = \bar{D} (1 + r)^2 \tag{19}$$

$$\bar{k}_{22} = -\bar{D} (1 + r)^4 \{\sinh(\alpha r) [\frac{1}{\alpha} - \frac{3}{\beta} + \frac{3}{\alpha\beta^2}] + \cosh(\alpha r) [1 - \frac{3}{\beta^2} - \frac{3}{\alpha\beta}]\},$$

where

$$\bar{D} = \frac{CGJ_a}{(\rho/CG)^{1/2}} [(\frac{1}{\alpha\beta} - 1) \sinh(\alpha r) - \frac{r}{\beta} \cosh(\alpha r)] \tag{20}$$

It is of interest to note that the torsional dynamic stiffness influence coefficient $\bar{D}_{ij}$, which are presented by Beskos et al. (1983) for a uniform element, can be deduced as a particular case of the $\bar{k}_{ij}$ given by equation (19) for $\alpha=\beta$ and r tending to zero.

EFFECT OF DAMPING

Both internal and external viscous damping can be accounted for by the transformed dynamic stiffness influence coefficients. For reasons of simplicity, the material of the bar is assumed to be a Kelvin solid obeying the constitutive law (Flugge 1967)

$$\sigma = W (\varepsilon + f \frac{d\varepsilon}{dt}), \tag{21}$$

where σ is the stress, ε is the strain, W represents either the modulus of elasticity E or the shear modulus G, and f is the damping coefficient. Equation (21) in the Laplane transform domain takes the form

$$\bar{\sigma} = W (1 + fs)\bar{\varepsilon} \tag{22}$$

which implies that internal viscous damping can be considered by replacing W with W(1+fs) in equations (6) and (15), respectively.

When external viscous damping is present, the additional damping force, R, is introduced in the equations of motion. Denoting with c the coefficient of damping, R can be expressed as

$$R = -c \frac{du}{dt} \tag{23}$$

Application of Laplace transform on equation (17) yields

$$\bar{R} = -cs\bar{u} \tag{24}$$

Expressions (22) and (24) indicate that equations (8) and (17) can account for combined external viscous and internal viscoelastic damping by replacing the variables a and α with a and α , respectively, where

$$a = \frac{sL}{r} \left(\frac{\rho}{E(1+fs)}\right)^{1/2} + cs \quad , \quad \alpha = \frac{sL}{r} \left(\frac{\rho}{CG(1+fs)}\right)^{1/2} + cs \qquad (25)$$

In contrast to the conventional way of accounting for damping as a percentage of the critical damping either in a mode superposition analysis or in a direct integration procedure, the present formulation allows the assignment of different damping properties for each individual structural member. As a result, the dynamic behavior of linear structures can be efficiently simulated in a more rational way.

FORMULATION OF THE PROBLEM

Once the dynamic stiffness coefficients are defined, the dynamic problem of a bar/shaft can be formulated in the following static-like form in the Laplace transform domain

$$\{\bar{F}(s)\} = [\bar{k}(s)] \{\bar{u}(s)\}, \qquad (26)$$

where $\{\bar{F}(s)\}$ and $\{\bar{u}(s)\}$ represent the Laplace transformed axial/torsional dynamic load and displacement vectors, respectively. After the transformed boundary conditions are applied, $\{\bar{u}(s)\}$ can be obtained from equation (26) by a matrix inversion of the dynamic stiffness matrix for a sequence of values of s. Then the response $\{u(t)\}$ in the time domain can be determined by a numerical inversion of the Laplace transformed displacement vector. The response $\{u(t)\}$ is the exact solution of the dynamic problem, since the dynamic stiffness matrices have been developed from the exact solutions of the transformed equations of motion.

The numerical algorithm adopted herein to invert the transformed response has been developed by Durbin (1974). It combines both finite Fourier cosine and sine transforms and operates with complex values of s. Thus, it is more time consuming than other algorithms operating with real data. Nevertheless, Durbin's algorithm has been chosen since it provides higher accuracy than real data algorithms, a feature which is crucial in dynamic problems involving excitations of a transient time variation.

The above formulation is based on the assumption of zero initial conditions. However, consideration of non-zero initial conditions does not present any difficulty. In this case, the Laplace transform of equation (4) yields

$$\xi^2 \bar{u}'' + m \xi \bar{u}' - \xi^2 \frac{\rho L^2}{Er^2} s^2 \bar{u} = \bar{q} (x,s) ,$$

$$\bar{q} (x,s) = - \frac{\rho L^2}{Er^2} \xi^2 [s u(x,o) + \dot{u}(x,o)] , \qquad (27)$$

where $u(x,o)$ and $\overset{\bullet}{u}(x,o)$ are the initial axial displacement and velocity of the axial element, respectively. Thus, the initial conditions in the Laplace transform domain can be represented by a load distributed along the length of the element. The distributed load can be converted to a vector of equivalent nodal forces $\{\overset{\bullet}{f}_i(s)\}$, $i = 1,2$, through standard finite element procedures (Davies 1980).

NUMERICAL EXAMPLES

This section presents the solutions of numerical examples in order to illustrate the method and demonstrate its merits. The numerical computations where performed on a IBM 3081-D computer.

EXAMPLE 1

Consider the structural system in figure 2 which consists of one tapered and one uniform bar with rectangular cross-sections having a constant width b. The numerical data pertaining to this system is L = 10 in (25.4 cm), b = 1.0 in (2.54
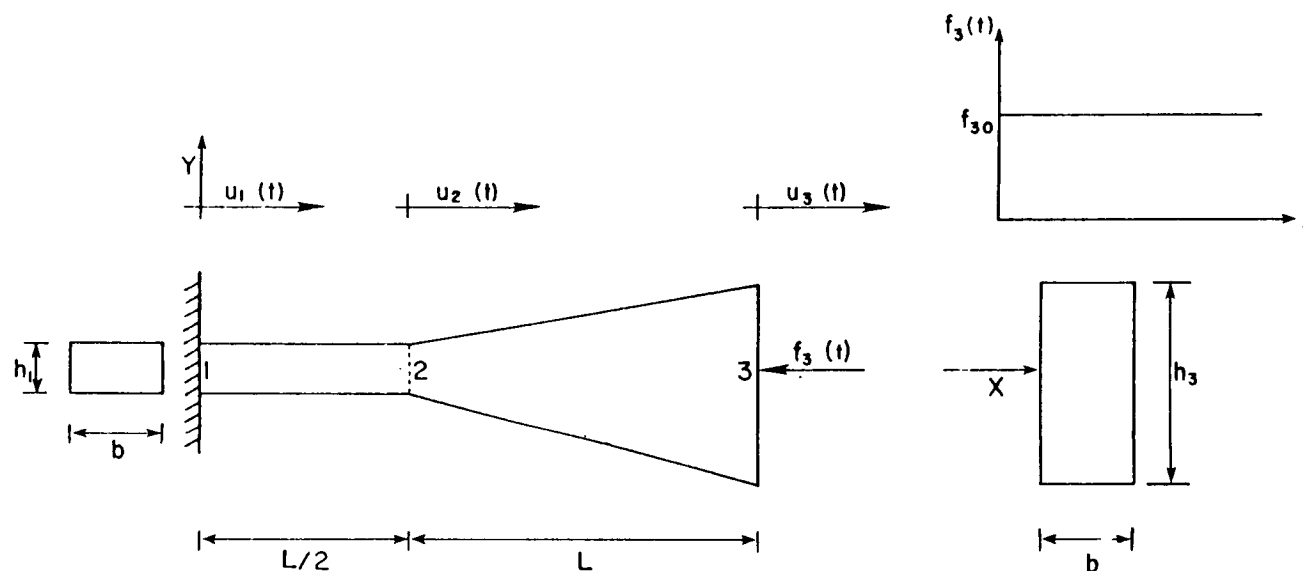

Fig. 2 Geometry and loading of the structural system of example 1

cm), $h_1 = h_2 = 0.5$ in (1.27 cm), $h_3 = 2.5$ in (6.35 cm), $\rho = 0.002$ lb-sec^2/in^4 (0.0214 kg/cm^3), $E = 10^7$ lb/in^2 (6.89x10^5 N/mm^2), and $f_{30} = 10^6$ lb (4.448x10^6 N). The values of the subscript i = 1,2,3 denote the element nodes as shown in figure 2. With the aid of the k_{ij} and the dynamic stiffness influence coefficients for a uniform bar (Beskos et al, 1983), $\overset{\bullet}{D}_{ij}$, the equilibrium equations in the frequency domain can be written in the form

$$
\left\{
\begin{array}{c}
\bar{f}_1(s) \\
0 \\
-\bar{f}_3(s)
\end{array}
\right\}
=
\left[
\begin{array}{ccc}
\bar{D}_{11} & \bar{D}_{12} & 0 \\
\bar{D}_{21} & \bar{D}_{22} + \bar{K}_{22} & \bar{K}_{12} \\
0 & \bar{K}_{21} & \bar{K}_{22}
\end{array}
\right]
\left\{
\begin{array}{c}
0 \\
\bar{u}_2(s) \\
\bar{u}_3(s)
\end{array}
\right\}
\tag{28}
$$

Equation (29) solved for $\bar{u}_3(s)$ yields

$$
\bar{u}_3(s) = -\bar{f}_3(s)\,[\bar{K}_{22} - \frac{(\bar{K}_{12})^2}{\bar{K}_{11} + \bar{D}_{22}}\,]^{-1}\,,
\tag{29}
$$

where

$$
\bar{D}_{22} = h_1 bEw/\tanh\,\frac{wL}{2}
\tag{30}
$$

with $\quad w = \dfrac{\rho s^2}{E}^{1/2}$

Evaluation of the Bessel functions appearing in the $\bar{k}_{ij}$ stiffness coefficients involve complex kernels with s ranging from very small to very large arguments. Thus, accurate evaluation of the $\bar{k}_{ij}$ requires use of appropriate assymptotic expansions of the modified Bessel functions $I_k(s)$ and $K_k(s)$ (Watson 1966).

The response $u_3(t)$ in the time domain is obtained by a numerical inversion using Durbin's algorithm and is plotted in figure 3. The total CPU time, including the formulation of equation (28), was only 0.14 secs. In order to establish the accuracy of the method, the $u_3(t)$ is also determined by the NASTRAN computer code using a mesh of twenty equal elements for the tapered bar and ten for the uniform member. The total CPU time required by NASTRAN was 26.87 secs. The present method required considerably less CPU time than NASTRAN, since it modelled the structure with one element per member. As shown in figure 3 the results obtained by NASTRAN and the present method are almost identical.
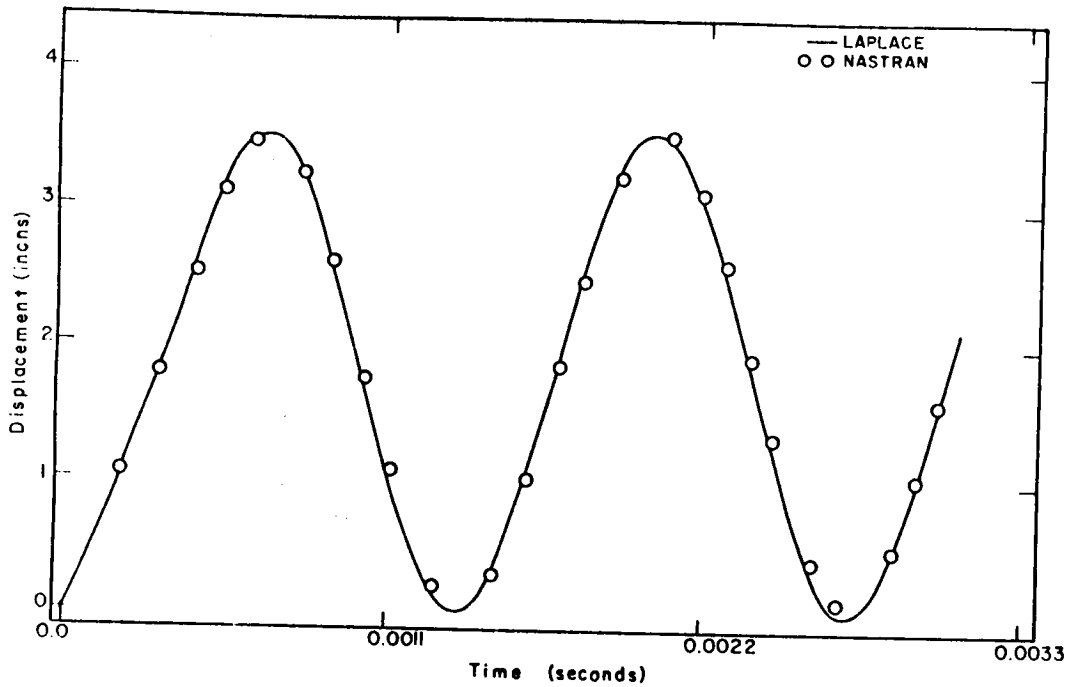
Fig. 3 Axial response $u_3(t)$ vs time of example 1

EXAMPLE 2

Consider the structural system of figure 4 that is composed of one tapered and one uniform shaft with circular cross-sections and subjected to a concentrated step torque of magnitude $T_{30} = 10^6$ lb-in (11.29×10^6 N-cm). The geometry of the structure is described by the parameters L = 10 in (25.4 cm), $R_1 = R_2 = 0.3989$ in (1.013 cm), $R_3 = 0.8921$ in (2.266 cm), q = 0.002 lb-sec²/in⁴ (0.0214 kg/cm³) and E = 10^7 lb/in² (6.89×10^5 N/mm²). The torque $-\bar{T}_3(s)$ acting at node 3 causes the torsional deformation $\bar{\Phi}_3(s)$ which can be evaluating from

$$\bar{\Phi}_3(s) = -\bar{T}_3(s) \left[\bar{K}_{22} - \frac{(\bar{K}_{12})^2}{\bar{K}_{11} + \bar{D}_{22}} \right]^{-1}, \tag{31}$$

where

$$\bar{D}_{22} = J_1 \quad GW \ [\tanh \ (\frac{WL}{2})]^{-1} \tag{32}$$

with

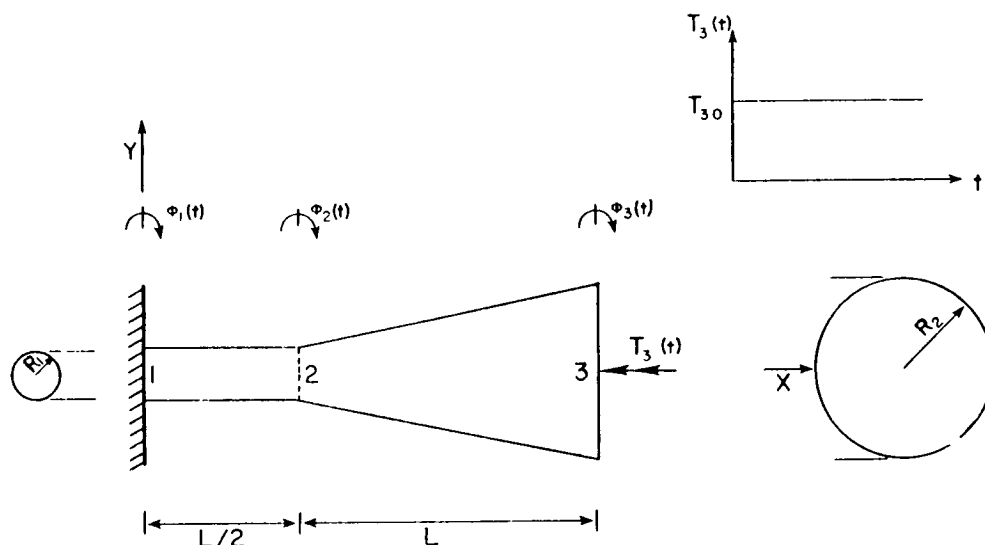$$W = \frac{\rho s^2}{2\pi R_1^2 G}^{1/2}$$

371

Fig. 4   Geometry and loading of the structural system of
example 2

In equations (32) the subscript 1 pertains to node 1 of the uniform shaft element.   Figure 5 shows the angular response $\Phi_3(t)$ in the time domain obtained by numerical inversion of $\bar{\Phi}_3(s)$.   The same figure also portrays results obtained by NASTRAN for a discretization of forty elements for the tapered shaft and ten for the uniform member.   The total CPU time required by NASTRAN was 38.23 secs, while the present method required only 0.09 secs. Evaluation of the angular response $\Phi_3(t)$ by the present method required less computational time than the evaluation of the axial response $u_3(t)$ in the first example.   This can be primarily attributed to the functional form of the $\bar{k}_{ij}$ and $\bar{k}_{ij}$ stiffness coefficients of equations (29) and (31), respectively.   The former are expressed in terms of Bessel functions, while the latter consists of hyperbolic functions.   It should be mentioned that results obtained by NASTRAN for a twenty element discretization of the tapered member did not provide sufficient accuracy.
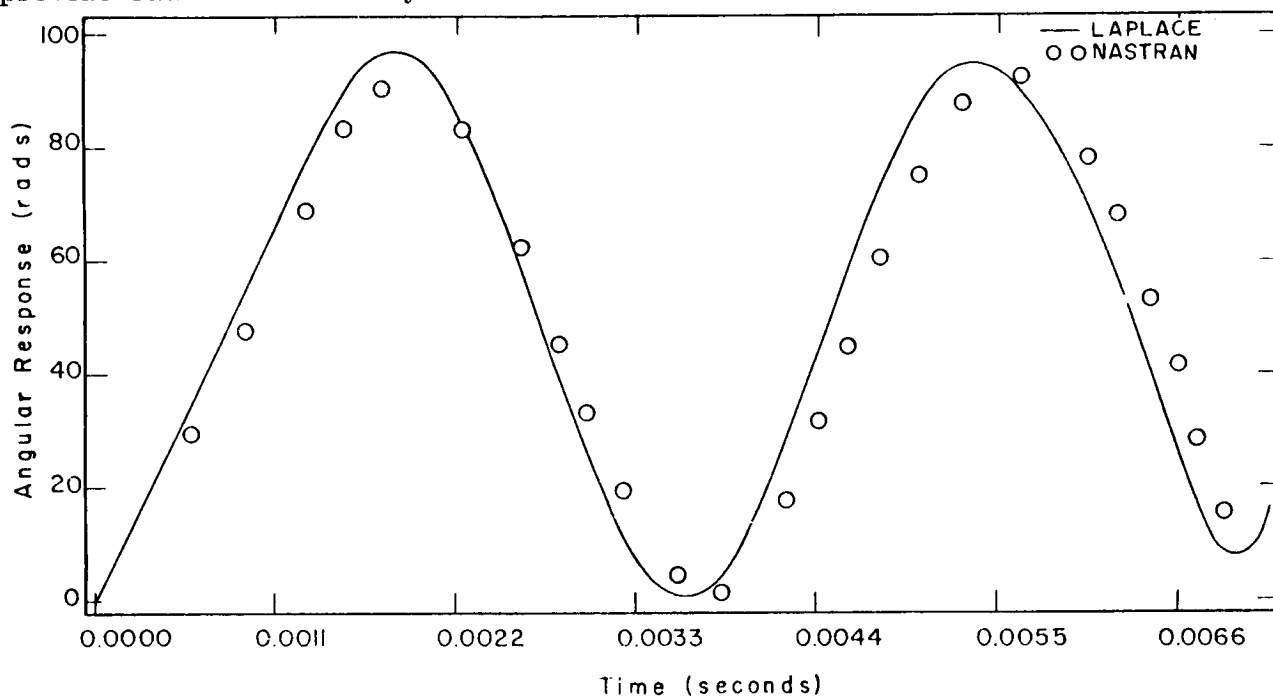

Fig. 5   Angular response $\Phi_3(t)$ vs time of example 2

CONCLUSIONS

In this work, the exact dynamic stiffness matrices of viscoelastic tapered bar and shaft elements are developed. These matrices can be incorporated in a finite element formulation to determine the response of structural systems to dynamic forces of a transient time variation. The formulation is performed in the Laplace transform domain resulting in a static-like relationship between the force and displacement vectors. The dynamic response is then obtained in the frequency domain numerically, and is subsequently evaluated in the time domain by a numerical inversion. Although the geometries and loading of the example problems presented are simple, the present method is general and applies to complicated situations.

Within the realm of assumptions and limitations of linear theories, the $\bar{k}_{ij}$ and $\bar{k}_{ij}$ dynamic stiffness coefficients lead to the "exact" solution of the problem, since they have been developed from the exact solutions of the transformed equations of motion. Thus, results obtained by the present method can be used to compare the accuracy of other numerical methods such as conventional finite element and finite differences methods.

Use of the $\bar{k}_{ij}$ and $\bar{k}_{ij}$ coefficients accounts for the inertia and stiffness properties of the system members accurately, through a modelling that requires only one element per member. This is a significant advantage of the proposed method over conventional finite element methods employing a lumped or a consistent mass representation. Further, the method does not require the evaluation of nodal shapes or eigenvectors. Any inaccuracy of results can be primarily attributed to the accuracy of the numerical inversion algorithm used.

The $\bar{k}_{ij}$ and $\bar{k}_{ij}$ coefficients permit consideration of different levels of external or internal viscoelastic damping at each one of the axial/torsional members, the supports and the joints. Thus, one can control the response through a more rational estimation of the damping attributed to the individual structural members.

REFERENCES

Abramowitz, M., and Stegan, I.E. (1965). Handbook of Mathematical Functions National Bureau of Standards, Washington, D.C.

Banerjee, J.R., and Williams R.W. (1986). "Exact Bernouli-Euler Dynamic Stiffness Matrix for a Range of Tapered Beams." International Journal for Numerical Methods in Engineering, Vol. 21, 2289-2302.

Bathe, K.J. (1982). Finite Element Procedures in Engineering Analysis. Prentice Hall, New Jersey.

Beaufait, F.W., Rowan, W.H. Hoadley, P.G., and Hackett, R.M. (1970) Computer Methods of Structural Analysis. Prentice Hall, New Jersey.

Beskos, D.E., and Narayanan, G.V. (1983). "Dynamic Response of Frameworks by Numerical Laplace Transform." Computer Methods in Applied Mechanics and Engineering, Vol. 37, 289-307.

Chu, F.H., and Pilkey, W.D. (1979). "Transient Analysis of Structural Members by the CSDT Riccati Transfer Matrix Method." Computers and Structures, Vol. 10, 599-611.

Davies, A.J. (1980). The Finite Element Method: A First Approach. Oxford University Press, London.

Durbin, F. (1974). "Numerical Inversion of Laplace Transform: An Efficient Improvement of Dudner and Abate's Method." The Computer Journal, Vol. 17, 371-376.

Flugge, W. (1967). Viscoelasticity. Blonsdell Publishing Company, Massachusetts.

Gallager, R.H., and Lee, C.H. (1970). "Static Dynamic and Stability Analysis with Non-Uniform Elements." International Journal for Numerical Methods in Engineering, Vol. 2, 265-275.

GangaRao, H.V.S., and Spyrakos, C.C. (1986). "Closed Form Series Solutions of Boundary Value Problems with Variable Properties." Computers and Structures, Vol. 23, No. 2, 211-215.

Gupta, A.K. (1985). "Vibration of Tapered Beams." Journal of the Engineering Mechanics Division, ASCE, Vol. 111, 19-36.

Holzer, S.M. (1985). Computer Analysis of Structures: Elsevier, New York.

Just, D.J. (1977). "Plane Frameworks of Tapering Box and I-section." Journal of the Structural Division, ASCE, Bol. 103, 71-86.
Kolonsek, V. (1973). Dynamics in Engineering Structures. Butterworths, London.

Kounadis, A.N. (1975). "Beam Columns of Varying Cross-section Under Lateral Harmonic Loads." Ingenieur-Archiv., Vol. 44, 43-51.

Liable, J.P. (1985). Structural Analysis. CBS College Publishing, New York.

Myers, J.E. (1971). Analytical Methods in Conduction Heat Transfer. McGraw-Hill, New York.

Rough, K.E., and Kao, J.S. (1979). "A Tapered Beam Finite Element for Rotor Dynamics." Journal of Sound and Vibration, Vol. 66, 119-149.

Sato, K. (1980). "Transverse Vibrations of Linearly Tapered Beams with Ends Restrained Elastically Against Rotation Subjected to Axial Force." International Journal of Mechanical Science, Vol. 22, 109-115.

Spyrakos, C.C., and Beskos, D.E. (1982). "Dynamic Response of Frameworks by Numerical Laplace Transform." Computers and Structures, Vol. 15, 495-505.

Tamma, K.K., Spyrakos, C.C., (1987) and Lambi, M.A. (1987). "Thermal/Structural Dynamic Analysis via a Transform Method Based Finite Element Approach." Journal of Spacecrafts and Rockets, AIAA, Vol. 24, No. 3, 219-226.

Watson, G.N. (1966). A Treatice on the Theory of Bessel Functions. Cambridge University Press, London.